

A new deterministic gasket fractal based on ball sets

Roberto Soto-Villalobos
Universidad Autónoma
de Nuevo León, Facultad
de Ciencias de la Tierra
Carretera a Cerro Prieto
km 8.0
67700, Linares, Mexico
roberto.sotovll@uanl.edu.mx
ORCID:0000-0002-3172-
8673

Francisco Gerardo
Benavides-Bravo
Tecnológico Nacional de
México, Instituto
Tecnológico de Nuevo
León
Av Eloy Cavazos 2001
67170, Guadalupe,
Mexico
francisco.bb@nuevoleon.tecnm.mx
ORCID:0000-0002-4596-
831X

Filiberto
Hueyotl-Zahuantitla
Cátedra
CONACyT-UNACH
Carretera Emiliano
Zapata km 8.0
29050, Tuxtla Gutiérrez,
Mexico
fhueyotl@conacyt.mx
ORCID:0000-0002-5527-
7141

Mario A. Aguirre-López*
Universidad Autónoma
de Chiapas, Facultad de
Ciencias en Física y
Matemáticas
Carretera Emiliano
Zapata km 8.0
29050, Tuxtla Gutiérrez,
Mexico
marioal1906@gmail.com
ORCID:0000-0002-5191-
3462
*Corresponding author

ABSTRACT

In this paper, we propose a new gasket fractal constructed in a deterministic iterated function system (IFS) way by means of interacting ball and square sets in \mathbb{R}^2 . The gasket consists of the ball sets generated by the IFS, possessing also exact self-similarity. All this leads to a direct deduction of other properties and a clear construction methodology, including a dynamic geometry procedure with an open-source construction protocol. We also develop an extended version of the fractal in \mathbb{R}^n . Some resulting configurations consisting of stacked 2D-fractals are plotted. We discuss about potential applications of them in some areas of science, focusing mainly on percolation models. Guidelines for future work are also provided.

Keywords

gasket fractal, n -sphere, iterated function systems, box-counting dimension, dynamical geometry, percolation

1 INTRODUCTION: BACKGROUND AND NOTATION

Fractals are geometrical shapes made up of smaller and smaller elements than add roughness to the entire shape. Talking about its length is not clear since there will always be something finer that will escape the sensitivity of the instrument used, increasing or decreasing this measurement. Then, they should be measured by borders, polygons, balls, boxes or new concepts that go beyond classical geometric concepts.

In other words, when we measure any shape by choosing different measurement scales, power law relationships written by $N = s^D$ are fulfilled, with N as the number of segmented figures, s the similarity dimension, and D the fractal dimension. If the shape satisfies the above relation with D as a

non-entire number, we are dealing with a fractal [B.B83]. Among those structures, gasket fractals are defined such as those ones that are constructed by joints of sets.

Gasket fractals have become a source of inspiration for the design of several digital and physical structures [Gua18, AHHN21, Rao21, FFSS22]. Some of the most popular fractals within this kind are generated by applying an iterated function system (IFS) to a deterministic formulation, such as the Koch snowflake [Koc04], the Sierpinski triangle [Sie15], the T-square [DJW16], the Cantor dust [Can70, Can71], and its two-dimensional and three-dimensional versions: the Sierpinski carpet [Sie16] and the Menger sponge [Edg04], respectively.

Our fractal design belongs to the the above sub-kind of construction. It is defined in an Euclidean space in \mathbb{R}^2 . Two types of sets are the basis of the generating IFS: on the one hand, $B(c, r)$ refers, as usual, to a closed ball with radius r that is centered at c , $r \in \mathbb{R}$, $c \in \mathbb{R}^2$; on the other hand, we refer by $S(c, r)$ to the set composed by all the points inside and on the borderline of a square, a "closed-square", with side $2r$ that is centered at c . In this way, both kind of sets B and S , are defined by

Permission to make digital or hard copies of all or part of this work for personal or classroom use is granted without fee provided that copies are not made or distributed for profit or commercial advantage and that copies bear this notice and the full citation on the first page. To copy otherwise, or republish, to post on servers or to redistribute to lists, requires prior specific permission and/or a fee.

their center position and radius of the maximum circumscribed circle inside the square. The paper is structured as follows: fractal's definition and its main properties are introduced in Section 2, for 2D and higher dimensions; the method of construction, both pseudo-code and procedure by dynamical geometry using open-source software, is detailed in Section 3; Section 4 exemplifies the potential applications of some resulting fractal arrangements and discuss about other potential uses; finally, concluding remarks and guidelines for future works are discussed in Section 5.

2 MODELING THE FRACTAL

Let the initial set $S(\kappa_0, \rho_0)$ and its largest circumscribed ball $B(\kappa_0, \rho_0) \equiv F_0$, $\kappa_0 \in \mathbb{R}^2$, $\rho_0 \in \mathbb{R}$. At the first iteration, $S(\kappa_0, \rho_0)$ is divided into the four largest squares $S(\kappa_i, \rho_1)$, $i = 1, 2, 3, 4$, each of them intersecting $B(\kappa_0, \rho_0)$ in only one point $x_i \in \mathbb{R}^2$, $\bigcap_{i=1}^4 x_i = \emptyset$. The couples of parameters defining each generated i -th square are obtained by the fulfillment of the following constraints:

$$\kappa_i \in S(\kappa_0, \rho_0), \quad \kappa_i \notin B(\kappa_0, \rho_0), \quad \bigcap_{i=1}^4 \kappa_i = \emptyset \quad (1)$$

$$\rho_1 = \frac{1}{2} \sup \left\{ \delta : \left(S(\kappa_i, \delta) \subset S(\kappa_0, \rho_0), \right. \right. \\ \left. \left. S(\kappa_i, \delta) \cap B(\kappa_0, \rho_0) = x_i \right) \right\}, \quad \forall \delta > 0. \quad (2)$$

Due to symmetry, all the generated squares $S(\kappa_i, \rho_1)$, $i = 1, 2, 3, 4$, have the same radius length ρ_1 , and are equidistant to the center of their generator square $S(\kappa_0, \rho_0)$ in direction to its vertices, going through its respective x_i , see the representation in Fig. 1. So, the sub-index for the radius length goes with the iteration number. All this leads to the respective generated balls $B(\kappa_i, \rho_1)$, $i = 1, 2, 3, 4$, which make up F_1 .

Now, this function system is extended to the m -th iteration, $m \geq 1$, by substituting $S(\kappa_0, \rho_0)$ with each j -th square generated at the $(m - 1)$ -th iteration, and applying Eqs. (1) and (2) to them. Since each new ball becomes a generator of four balls of lower size but possessing the property of exact self-similarity, we can easily calculate that generated number of balls $N_m = 4^m$ balls with radius $\rho_m = \rho_0 u^m$, with $u = (1 - \sqrt{2}/2)/2$, at the m -th iteration. Those power-law behaviors are shown in a logarithmic view in Fig. 2.

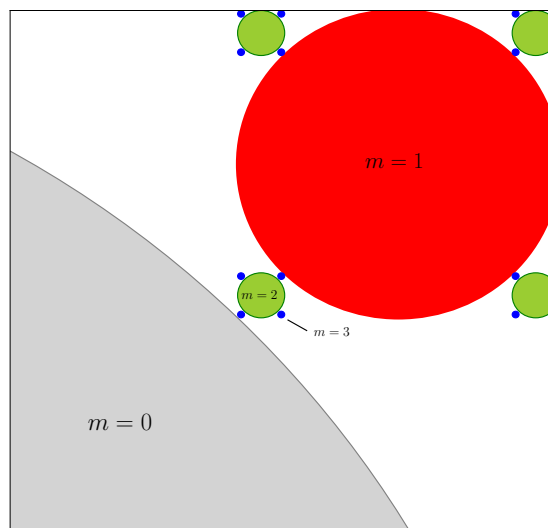


Figure 1: Top-right view of the fractal, the first three iterations are shown. The initial ($m = 0$) circumscribed gray ball $B(\kappa_0, \rho_0)$ generates four squares as described in the text, each of which leads a new level ($m = 1$) of circumscribed red balls $B(\kappa_{1,4}, \rho_1)$. Each red ball generates a new level ($m = 2$) of squares with their respective circumscribed green balls $B(\kappa_{5:20}, \rho_2)$. The process continues taking the green balls as generators, four blue balls ($m = 3$) generates for each green ball, and so on.

Other properties, such as the cumulative area A_m and the fractality D of the gasket can be directly calculated from ρ_m and N_m . Namely:

$$A_m = \sum_{i=0}^m N_i \pi (\rho_i)^2 = \pi (\rho_0)^2 \sum_{i=0}^m 4^i u^{2i}, \quad (3)$$

being the last expression in terms of the initial radius ρ_0 . Then, taking $m \rightarrow \infty$ and normalizing Eq. (3) with respect to $S(\kappa_0, \rho_0)$, it becomes

$$A = \left(\frac{1}{(2\rho_0)^2} \lim_{m \rightarrow \infty} A_m \right) \times 100\% \approx 86\%. \quad (4)$$

In turn, since our gasket is deterministic and exact self-similar, the fractal dimension can be computed by a simple formula related to the box-counting formulation [Fal90]:

$$D = \frac{\ln v}{\ln \frac{1}{u}} = \frac{\ln 4}{\ln \frac{2}{1-\sqrt{2}/2}} = 0.72, \quad (5)$$

where v takes its value from the number of balls generated per square. In this way, the fractality of our gasket is lower than other known 2D self-similar gaskets, such as the Sierpinski triangle ($D_{ST} = 1.59$), the Sierpinski carpet ($D_{SC} = 1.89$),

the T-square ($D_{T-square} = 1.58$), and the Koch curve ($D_{Koch} = 1.26$). Indeed, it has a fractal dimension about the 1D Cantor dust ($D_{Cantor} = 0.63$).

Definition. Let $F_{m,q}$, the q -th ball generated at the m -th iteration of the IFS described above, then

$$F_m = \bigcup_{q=1}^{4^m} F_{m,q} \quad (6)$$

and the ball-gasket fractal consists of

$$F = \lim_{m \rightarrow \infty} F_m. \quad (7)$$

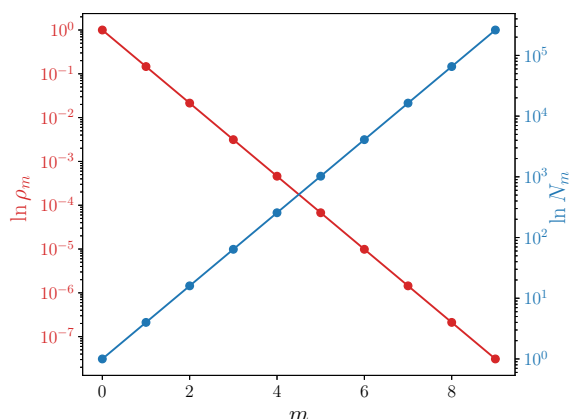


Figure 2: In red- logarithm on the radius ρ_m of the circumscribed balls as a function of the number of iterations m , assuming $\rho_0 = 1$. In blue- logarithm of the number of generated balls N_m in each iteration m .

Extension to \mathbb{R}^n

The construction method of F allows to formulate it for an euclidean space in \mathbb{R}^n . The first step is to extend our definitions for squares and balls to $S^n(c, r)$ and $B^n(c, r)$, in which they refer to the set of points inside an n -cube and an n -sphere, respectively, centered at $c \in \mathbb{R}^n$ and having radius $r \in \mathbb{R}$, i.e., the nomenclature for the original case in \mathbb{R}^2 would be $S^2(c, r)$ and $B^2(c, r)$.

Then, the number of the generated n -spheres depends on the number of vertices of the n -cubes: 2^n for the n -dimensional case [Cox74], so that a total of $N_m^n = 2^{nm}$ balls are generated at the m -th iteration, each one with different intersection point $x_i \in \mathbb{R}^n$, $\bigcap_{i=1}^{2^n} x_i = \emptyset$, and Eq. (1) becoming

$$\kappa_i \in S(\kappa_0, \rho_0), \quad \kappa_i \notin B(\kappa_0, \rho_0), \quad \bigcap_{i=1}^{2^n} \kappa_i = \emptyset. \quad (8)$$

Thus, our n -dimensional ball-gasket fractal is denoted by

$$F^n = \lim_{m \rightarrow \infty} F_m^n, \quad (9)$$

where

$$F_m^n = \bigcup_{q=1}^{2^{nm}} F_{m,q}^n, \quad (10)$$

and $F_{m,q}^n$ represents q -th ball generated at the m -th iteration.

Finally, since the number of generated balls per iteration changes with n but not the ball radius, the properties of the fractal must be also re-calculated for the n -dimensional case:

$$A_m^n = \sum_{i=0}^m N_i^n \frac{\pi^{n/2} (\rho_i)^n}{\Gamma(n/2 + 1)} = \frac{\pi^{n/2} (\rho_0)^n}{\Gamma(n/2 + 1)} \sum_{i=0}^m 2^{ni} u^{ni}, \quad (11)$$

where $\Gamma(\cdot)$ is the Euler's gamma function, and the second factor in the sum computes the area of an n -sphere [NIS]. In turn, the box-counting dimension for the n -dimensional case (D^n) changes with the number of generated n -sphere per each n -cube (v^n), so that

$$D^n = \frac{\ln v^n}{\ln \frac{1}{u}} = \frac{\ln 2^n}{\ln \frac{2}{1-\sqrt{2}/2}}. \quad (12)$$

3 METHODOLOGY FOR 2D CONSTRUCTION

The pseudo-code for the F^2 's construction is shown in Algorithm 1, according to the definition introduced in Section 2. The algorithm is designed in such a way that it not only draws the fractal (line 19) but saves the information of each generated circle, such as its radius (line 10), center (lines 15:18), and area (lines 6,21-22). Then, the outputs are the fractal F^2 , its parameters κ_0 :index, ρ_0 :m, and the normalized cumulative area A .

In turn, Algorithm 2 presents a set of steps to generate F_1^2 , up to the 1-st iteration, based on dynamic geometry via the open-source software Geogebra [HBA⁺13]. This way of construction could be reached with using only the eight buttons shown in Fig. 3, so that it is useful for educational purposes. Fig. 4 also illustrates the fractal up to $m = 1$, while the reader could refer to the *Supplementary material* for the construction protocol to generate it up to the 3-th iteration, taking $\rho_0 = 1$ units and $\kappa_0 = (0, 0)$.

Algorithm 1 Pseudo-code for F^2

```

1: procedure GENERATOR OF  $F^2(\kappa_0, \rho_0)$ 
2:   System Initialization ▷ Set  $m$ 
3:   Read the entry values
4:   newBalls=1 ▷ Balls at  $m = 0$ 
5:   index=newBalls ▷ cumulative count
6:    $A = 1$  ▷ Initialize the norm. cum. area
7:   for  $i$  in 1: $m$  do ▷ Start the iterations
8:     lastBalls=newBalls ▷ Generators
9:     newBalls= $4^i$  ▷ To generate
10:     $\rho_i = \rho_0 u^i$ 
11:    for  $j$  in 1:lastBalls do ▷ Start to generate
12:       $G = \text{index} - \text{lastBalls} + j$ 
13:       $k = \text{index} + 4(j - 1)$ 
14:       $\delta = \rho_{i-1} - \rho_i$ 
15:       $\kappa_{k+1}^x = \kappa_G^x + \delta; \kappa_{k+1}^y = \kappa_G^y + \delta$ 
16:       $\kappa_{k+2}^x = \kappa_G^x - \delta; \kappa_{k+2}^y = \kappa_G^y + \delta$ 
17:       $\kappa_{k+3}^x = \kappa_G^x - \delta; \kappa_{k+3}^y = \kappa_G^y - \delta$ 
18:       $\kappa_{k+4}^x = \kappa_G^x + \delta; \kappa_{k+4}^y = \kappa_G^y - \delta$ 
19:      Draw  $B(\kappa_{k+l}, \rho_i)$  ▷ for  $l = 1 : 4$ 
20:    index=index+newBalls
21:     $A = A + 4^i u^{2i}$  ▷ Computing with Eq. (3)
22:     $A = \frac{\pi A}{4} \times 100\%$  ▷ Normalizing with Eq. (4)
23:  output:  $F^2, \kappa_0; \text{index}, \rho_0; m, A$ 

```

Algorithm 2 Construction of F_1^2 in GeoGebra.

```

1: procedure GENERATOR OF  $F_1^2(\kappa_0, \rho_0)$ 
2:   System Initialization ▷ Use
   the command SetAxesRatio(1,1) in order
   to fix a scale 1:1
3:   Draw a square centered at  $\kappa_0$  with side  $2\rho_0$ ,
   using button a) ▷
   Generating the points  $(-\rho_0, \rho_0) + \kappa_0, (\rho_0, \rho_0) +$ 
 $\kappa_0, (\rho_0, -\rho_0) + \kappa_0, (-\rho_0, -\rho_0) + \kappa_0$ 
4:   Draw a polygon using button b) ▷
   By joining all the previous points, starting and
   ending at the same point
5:   Find a midpoint of any side of the square
   with button c)
6:   Using button d), draw a circle with  $\kappa_0$  as its
   center, and the radius of the midpoint found
   previously
7:   Draw the diagonals of the square with but-
   ton e) ▷ At this step, the resulting picture is
   shown in Fig. 4 (a)
8:   Find the intersections of the circle with the
   diagonals with button f)
9:   Draw the perpendicular bisectors between
   the corners of the square and the intersections
   of the diagonal with the circle by means of but-
   ton g)
10:  Find the intersections of the sides of the
   square with the perpendicular bisectors using
   button f)
11:  Reflect the square corresponding to the 1st
   quadrant up to generate the rest of the new
   squares with button h). ▷ The resulting
   picture is shown in Fig. 4 (b).
12:  Note: To continue up to the  $i$ -th iteration,
   repeat steps 4 to 10 for the generated circles,
   substituting  $\kappa_0$  and  $\rho_0$  with the correspond-
   ing center and radius of each generated circle.
   Then continue to Step 11.

```

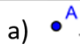
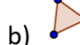
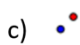
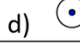
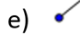
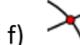
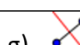
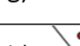
a) 	Point
b) 	Polygon
c) 	Midpoint or Center
d) 	Circle with Center through Point
e) 	Segment
f) 	Intersect
g) 	Perpendicular Bisector
h) 	Reflect about line

Figure 3: Table of buttons used for the geometrical construction in Geogebra.

4 RESULTING CONFIGURATIONS AND POTENTIAL APPLICATIONS

Although the objective of this work is not to delve into a direct application of the fractal, in this section we provide the reader some potential lines of research in which it could be used.

4.1 Stacked sets for percolation

Since its squared delimitation, diverse structured configurations or arrangements can be obtained from stacking F^2 sets. Fig. 5 (a) shows the most basic stack, which consists of an intersected structured in multiple scales. Indeed, each main generator ball $B(\kappa_0, \rho_0)$ touches its four-nearest similar

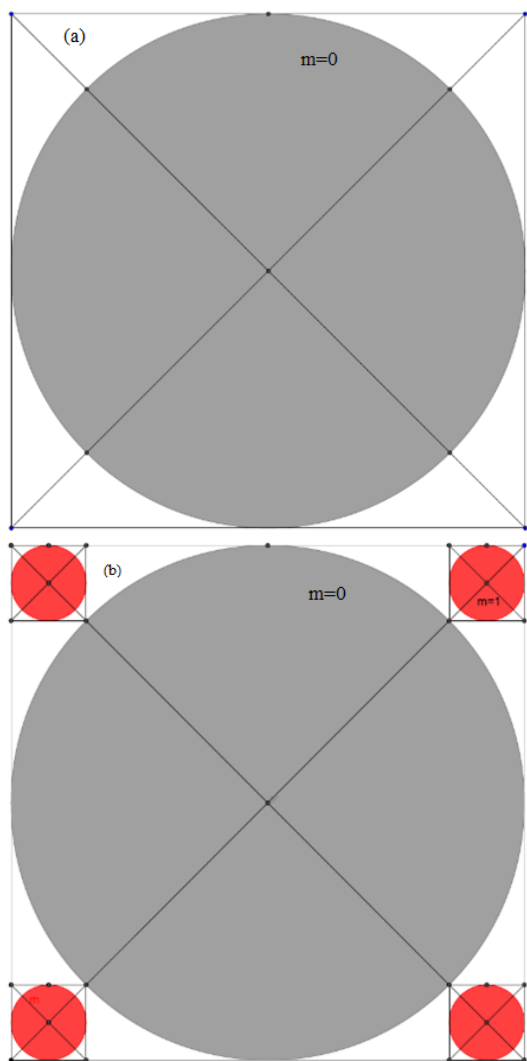


Figure 4: Geometrical construction in Geogebra. (a) Steps up to $m = 0$. (b) Steps up to $m = 1$.

neighbors; for the i -th iteration, $i > 0$, the generated balls in a corner of its main generator square ($S'(\kappa_0, \rho_0)$) touch their two-nearest similar neighbors from their corresponding main generators; in turn, the generated balls that are in contact with the border of its generator square, without being in a corner, touch only one similar neighbor.

In percolation terms, picture in Fig. 5 (a) defines a 2D slice of a porous but not-permeable structure (in the shown 2D slice) at different scales. Intact granite is a rock example that approximates to those characteristics [SBN05]. In the same line, Fig. 5 (b) shows an alternative configuration consisting of an overlapping of the fractals of Fig. 5 (a), by matching their nearest corners at their 1-st iteration. This also reduces porosity, because of the contraction of the stack, allowing variation in the modelling.

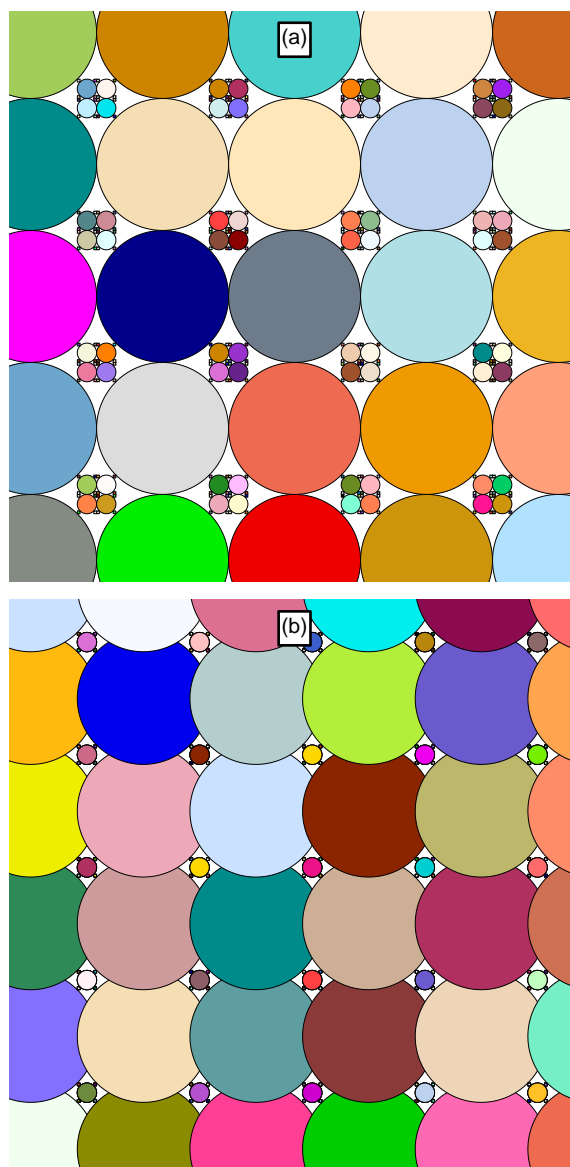


Figure 5: Porous and non-permeable stacks of fractals plotted with random colors up to the 3-rd iteration. (a) Most basic configuration. (b) Implementing an overlapping at the 1-st iteration.

Now, permeability could be introduced under the same reasoning by:

- adding a translation (ϕ) to interspersed lines of the stack, like that with $\phi = \rho_0/2$ in upward direction shown in Fig. 6 (a). Different from pictures in Fig. 5, this configuration only allows connected with two neighbors between main generators, while the rest of the balls do not touch each other, leading to a low permeability in mainly one direction but remaining the filled area in 86%. Similar structures are found in cracked crystalline rocks [NM14], and clay sediments making non-permeable beds [Car39].

- randomly selecting some balls not to draw. This leads to unknown paths of interconnected porous, reducing the filling area in dependence on the probability of drawing (p). Fig. 6 (b) shows an implementation of that kind of configuration with $p = 0.5$, which could be adaptable to make several shapes according to the geological structure to simulate or characterize. It could be useful for the case of sandstone, whose permeability depends of its relative composition [ZSDL15].
- a combination of the techniques mentioned previously.

In contrast to similar fractal models, like the space-filling packing from inversion of circles/spheres, that leave no porosity on the limit of infinitesimally small spheres [Ley05, SH18], our original fractal is a porous structure even in the limit, and can be easily modified to adjust the level of porosity.

Based on the above, our fractal would serve as a basis model for 2D or 3D rendering of rocks with a similar structure and/or fractal dimension, applying it as a direct modeling after the characterization of the rock [LWXY⁺22]. That methodology has been implemented previously to construct tessellations from iterative rules but not involving fractals [NM14, LMH10]. So, it could be a novel variation to improve that methodology, expecting some advantages such as the quick construction, and easy and deterministic control of the minimum-maximum size (by the iterations number). Nevertheless there are some limitations such as the fixed location and size of new circles, at the current version of our fractal, without modifying it or adding noise.

Figs. 5 and 6 were drawn by implementing the pseudo-code of Algorithm 1 in Rstatistics software [R C21].

4.2 Potential uses

In practice, the fractal dimension can also be determined by using the square side instead of the ball radius in Eqs. (5) and (12), leading to $D = 1.13$ and $D = 1.69$ for an extension to 3D. In this section we mention some similar dimensions and possible uses of our fractal. It is interesting that our fractal dimension is close to the value obtained ($D = 1.08 \pm 15$) by [Nos93], who indicates that the reason of the power-law form of the radio emission spectrum can be due to the fractal nature of the spatial distribution of radiating electrons; the value is also close to the fractal dimension of the perimeter ($D \sim 1.35$) of molecular clouds

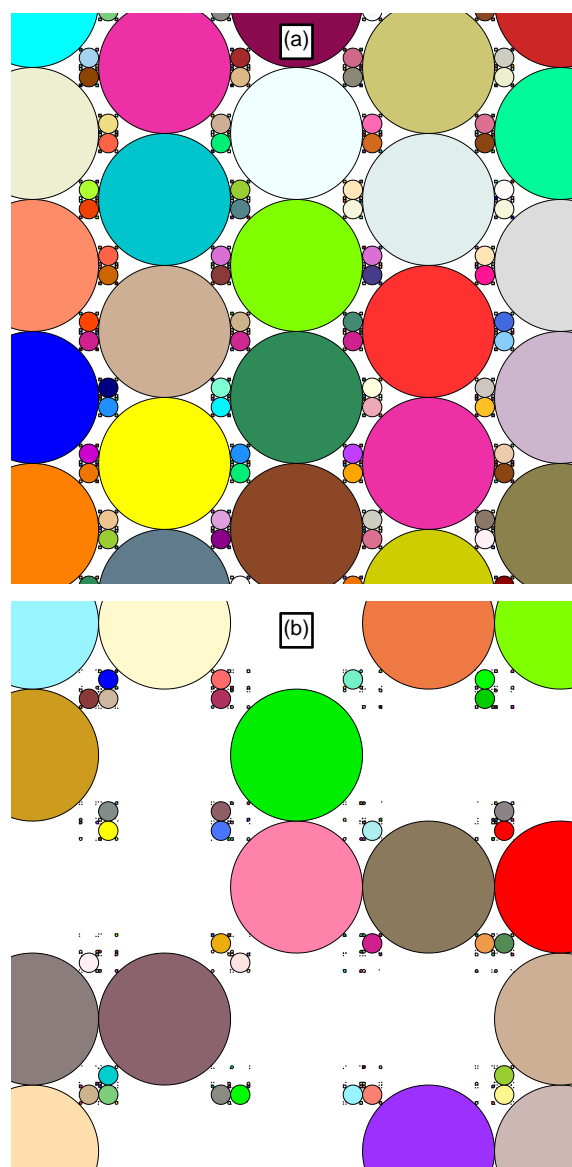


Figure 6: Porous and permeable stacks of fractals plotted with random colors up to the 3-rd iteration. (a) Structured modification applying a translation of $\phi = \rho_0/2$ in upward direction to interspersed lines. (b) Random modification by adding a probability of drawing $p = 0.5$ to each ball.

from two-dimension maps, see [SAP05] and references therein. These similarities on the fractal dimension suggest a similar level of roughness or sponginess, fact that could be useful to set conditions for modeling the phenomenon in the corresponding parameter space.

On the other hand, the relative low value of our dimension fractal is close to value, $D \sim 1.0 - 1.1$, for the corrosion-induced cracks in reinforced concrete (see, [JJZ⁺20]). In this case, variants of our fractal, as these in previous section, can have potential use to model different types of coarse ag-

gregate distribution to analyze (or even prevent) crack patterns. Last, but not least important is that our fractal could be taken as basis to generate garment geometrical patterns for clothing fabrics as in [Lam17] and [WZYW19]; furthermore, the 3D version could be used as an scene, like the sphere-flake used by [KML16], to test rendering methods. Here it is important to mention the existence of meshes based on fractals, some of them implemented in methodologies like the Delaunay triangulation using the Sierpiński triangle [BC92], and other ones exploring how phenomena occur with the developed fractal array, based on the Cantor set [SIK17]. In this sense, our fractal is more related to the latter one, due to the gaps in the filling space.

Finally, let the above mentioned potential uses, it is important to mention two particular characteristics of the fractal:

- It is difficult to appreciate the aesthetics of the fractal because the radius decreases almost one order in magnitude per iteration, see Fig. 2, so that the generated balls quickly disappear to the human-eye.
- the entire space is not fully filled, $A = 86\%$, this could be an advantage or disadvantage according to its use, and also contrast to others fractals involving a ball construction, such as the Apollonian fractal [Bou06].

5 CONCLUSIONS AND FUTURE WORK

We introduced a new gasket fractal consisting of 2D-balls embedded in squared sets, and constructed by means of a deterministic IFS. The fractal is exact-self similar, with a normalized cumulative area of 86%, and a box-counting dimension of $D = 0.72$, which differs from several well-known 2D fractals. Additionally, the gasket has the property of extend itself to \mathbb{R}^n while preserving a similar formulation to calculate its properties.

Beyond its limitations, our fractal possesses useful features that allow to apply it to diverse areas. In this way, we recommend to explore its fitting to represent percolation models and other topics inside numerical computational geometry.

Additionally to its applications, our gasket construction lays the basis for the definition of square-shaped fractals that are involved in the IFS of this work. A fractal composed of the generator squares, and two more based on the centers κ_i and in the intersection points x_i , are some examples of possible future lines of research.

ACKNOWLEDGMENTS

F.H.-Z. thanks FCFM-UNACH and the support from CONACyT through the program “Investigadoras e investigadores por México”, Cátedra 873. M.A.A.-L. thanks CONACyT for the postdoctoral grant 839412 and FCFM-UNACH for supporting his research stay.

6 REFERENCES

- [AHHN21] Ruaa Shallal Abbas Anooz, Ghufuran M Hatem, Iman Hafedh Yaseen Hasnawi, and Mohammed N Nemah. Design apollonian gasket antenna for millimeter-wave applications. *IOP Conference Series: Materials Science and Engineering*, 1094(1):012038, feb 2021.
- [B.B83] Mandelbrot B.B. *The Fractal Geometry of Nature*. W.H. Freeman, 1983.
- [BC92] S. W. Bova and G. F. Carey. Mesh generation/refinement using fractal concepts and iterated function systems. *International Journal for Numerical Methods in Engineering*, 33(2):287–305, 1992.
- [Bou06] Paul Bourke. An introduction to the apollonian fractal. *Computers & Graphics*, 30(1):134–136, 2006.
- [Can70] G. Cantor. Beweis, daß eine für jeden reellen werth von x durch eine trigonometrische reihe gegebene function $f(x)$ sich nur auf eine einzige weise in dieser form darstellen läßt, part 1. *Journal für die reine und angewandte Mathematik*, 72:139–142, 1870.
- [Can71] G. Cantor. Beweis, daß eine für jeden reellen werth von x durch eine trigonometrische reihe gegebene function $f(x)$ sich nur auf eine einzige weise in dieser form darstellen läßt, part 2. *Journal für die reine und angewandte Mathematik*, 73:294–296, 1871.
- [Car39] P. C. Carman. Permeability of saturated sands, soils and clays. *The Journal of Agricultural Science*, 29(2):262–273, 1939.
- [Cox74] H.S.M. Coxeter. *Regular complex polytopes*. Cambridge University Press, 1974.
- [DJW16] Nell Dale, Daniel T. Joyce, and Chip Weems. *Object-Oriented Data Structures Using Java*. Jones & Bartlett Learning, 2016.

- [Edg04] Gerald A. Edgar. *English translation of: "K. Menger (1926), Allgemeine Räume und Cartesische Räume. I., Communications to the Amsterdam Academy of Sciences"*. Westview Press, 2004.
- [Fal90] Kenneth Falconer. *Fractal geometry: mathematical foundations and applications*. John Wiley, 1990.
- [FFSS22] Z. Fair, M. Flanner, A. Schneider, and S. M. Skiles. Sensitivity of modeled snow grain size retrievals to solar geometry, snow particle asphericity, and snowpack impurities. *EGU-sphere*, 2022:1–22, 2022.
- [Gua18] Emanuel Guariglia. Harmonic sierpinski gasket and applications. *Entropy*, 20(9), 2018.
- [HBA⁺13] M. Hohenwarter, M. Borchers, G. Ancsin, B. Bencze, M. Blossier, A. Delobelle, C. Denizet, J. Éliás, Á Fekete, L. Gál, Z. Konečný, Z. Kovács, S. Lizelfelner, B. Parrisé, and G. Sturr. GeoGebra 4.4, December 2013. <http://www.geogebra.org>.
- [JJZ⁺20] Haodong Ji, Haoyu Jiang, Ruoyi Zhao, Ye Tian, Xianyu Jin, Nanguo Jin, and Jing Tong. Fractal characteristics of corrosion-induced cracks in reinforced concrete. *Materials*, 13:3715, 08 2020.
- [KML16] Kevin Keul, Stefan Müller, and Paul Lemke. Accelerating spatial data structures in ray tracing through pre-computed line space visibility. In *WSCG 2016 - 24th Conference on Computer Graphics, Visualization and Computer Vision 2016*, pages 17–25, 2016.
- [Koc04] H.V. Koch. Sur une courbe continue sans tangente, obtenue par une construction géométrique élémentaire. *Arkiv for Matematik, Astronomi och Fysik*, 1:681–704, 1904.
- [Lam17] Artde Donald Kin-Tak Lam. A study on fractal patterns for the textile design of the fashion design. In *2017 International Conference on Applied System Innovation (ICASI)*, pages 676–678, 2017.
- [Ley05] Jos Leys. Sphere inversion fractals. *Computers & Graphics*, 29(3):463–466, 2005.
- [LMH10] Hengxing Lan, C. Derek Martin, and Bo Hu. Effect of heterogeneity of brittle rock on micromechanical extensile behavior during compression loading. *Journal of Geophysical Research: Solid Earth*, 115(B1), 2010.
- [LWXY⁺22] Wei Lin, Zhenkai Li Wu, Zhengming Xizhe Yang, Mingyi Hu, Denglin Han, Chenchen Wang, and Jizhen Zhang. Digital characterization and fractal quantification of the pore structures of tight sandstone at multiple scales. *Journal of Petroleum Exploration and Production Technology*, 12:2565–2575, 2022.
- [NIS] NIST Digital Library of Mathematical Functions. 5.19 mathematical applications. Accessed: December 27, 2022.
- [NM14] M. Nicksiar and C.D. Martin. Factors affecting crack initiation in low porosity crystalline rocks. *Rock Mechanics and Rock Engineering*, 47:1165–1181, 2014.
- [Nos93] M. D. Noskov. Influence of the fractal nature of the spatial distribution of radiating electrons on a cosmic radio emission spectrum. *Astronomy Reports*, 37(5):565–566, September 1993.
- [R C21] R Core Team. *R: A Language and Environment for Statistical Computing*. R Foundation for Statistical Computing, Vienna, Austria, 2021.
- [Rao21] Nukala Srinivasa Rao. Design and analysis of koch snowflake geometry with enclosing ring multiband patch antenna covering s and l band applications. In Vijay Nath and J.K. Mandal, editors, *Nanoelectronics, Circuits and Communication Systems*, pages 167–176, Singapore, 2021. Springer Singapore.
- [SAP05] Néstor Sánchez, Emilio J. Alfaro, and Enrique Pérez. The fractal dimension of projected clouds. *The Astrophysical Journal*, 625(2):849, jun 2005.
- [SBN05] A. Selvadurai, M. Boulon, and T. Nguyen. The permeability of an intact granite. *Pure and Applied Geophysics*, 162:373–407, 2005.
- [SH18] D. V. STÄGER and H. J. HERRMANN. Self-similar space-filling sphere packings in three and four dimensions. *Fractals*, 26(03):1850022, 2018.
- [Sie15] Waclaw Sierpiński. Sur une courbe

- dont tout point est un point de ramification (in french). *Comptes rendus de l'Académie des Sciences*, 160:302–305, 1915.
- [Sie16] Waclaw Sierpiński. Sur une courbe cantorienne qui contient une image biunivoque et continue de toute courbe donnée (in french). *Comptes rendus de l'Académie des Sciences*, 162:629–632, 1916.
- [SIK17] Trifce Sandev, Alexander Iomin, and Holger Kantz. Anomalous diffusion on a fractal mesh. *Phys. Rev. E*, 95:052107, May 2017.
- [WZYW19] Weijie Wang, Gaopeng Zhang, Lum-ing Yang, and Wei Wang. Research on garment pattern design based on fractal graphics. *Eurasip journal on image and video processing*, 2019(1):1–15, 2019.
- [ZSDL15] Liwei Zhang, Yee Soong, Robert Dilmore, and Christina Lopano. Numerical simulation of porosity and permeability evolution of mount simon sandstone under geological carbon sequestration conditions. *Chemical Geology*, 403:1–12, 2015.